

SUPERCONDUCTIVITY IN THE QUATERNARY INTERMETALLIC
COMPOUND $YNi_{2-x}T_xB_2C$

Morgan E. Ware, PhD¹, William A. Mendoza, PhD², Prof. Dr. Shahid A. Shaheen³

¹College of Engineering, University of Arkansas, Fayetteville, AR 72701 USA

²*Florida State College at Jacksonville, Jacksonville, FL 32246 USA

³Department of Physics and Center for Materials Research and Technology (MARTECH), Florida State University, Tallahassee, FL 32306, USA

*Corresponding Author: w.a.mendoza@fscj.edu This work was undertaken with partial funding from the National Science Foundation of the USA in the laboratory of the late Prof. Dr. S. A. Shaheen.

We report here our observance of superconductivity in compounds derived from the quaternary intermetallic superconductor YNi_2B_2C by partial substitutions for Ni. Other 3d transition metals $T \in \{Ti, V, Cr, Mn, Fe, Co, Cu, Zn\}$ were used in replacement fractions $x = 0.05$ and $x = 0.10$. AC magnetic susceptibility χ_{AC} showed all except $T = Zn$ had the characteristic diamagnetic response seen in superconductors. DC SQUID magnetometry on several samples confirmed type II superconducting behavior. X-ray diffraction showed a crystal structure similar to the parent compound for all but $T = Zn$. Some of the $x = 0.10$ compounds appeared to have minor secondary phases present despite annealing.

I. INTRODUCTION

Quaternary intermetallic compounds of R-T-B-C borocarbide type where R is a rare earth metal (Y, Ho-Lu) and T is a transition metal (Pd or Ni) previously have been shown to superconduct at critical temperature (T_C) values of 23 K and below in bulk samples [1, 2]. For T = Ni, samples of YNi_4B , $YNi_4BC_{0.2}$, and $YNi_2B_3C_{0.2}$ showed superconductivity with T_C in the 12.5 to 13.5 K range [3, 4] but the superconducting phase of the borocarbides is now believed to be YNi_2B_2C [1]. Annealed samples of composition YNi_2B_2C were of single phase with $T_C = 15.6$ K [1]. Analysis of a $LuNi_2B_2C$ sample revealed a simple, layered crystal structure of the $I4/mmm$ space group (a filled variant of the body-centered tetragonal $ThCr_2Si_2$ structure) with alternating LuC and Ni_2B_2 planes [5]. Strong bond formation between the carbon and rare earth atoms results in the R-C planes, which alternate with the Ni-B planes. This structure allows the formation of multiple planes of Ni_2B_2 or the substitution of other 3d metals for Ni. Ordinarily, the presence of a ferromagnetic 3d metal would depress T_C in a superconductor, as local scattering centers from conduction electron spin-3d spin coupling form, but that does not appear to happen with YNi_2B_2C [1]. To examine these issues further, we prepared (i) a compound series with incremental 3d metal substitutions for Ni in YNi_2B_2C , and (ii) compounds of type YNi_xB_xC with $x \in \{2, 3, 4, 5\}$ to determine the effect of additional Ni_2B_2 planes.

II. EXPERIMENT

The $YNi_{2-x}T_xB_2C$ compounds with $T \in \{Ti, V, Cr, Mn, Fe, Co, Cu, Zn\}$ and $x = 0.05$ and 0.10 ($x = 0.05$ only for $T = Zn$) were prepared from high purity (99.9 wt %) metals, boron (99.5 wt %), and carbon (99 wt %). Stoichiometric amounts of elements were obtained using a Fisher XA-200DS electronic balance. The mixture was melted on a copper hearth in a water-cooled Centorr tri-arc furnace under a flowing argon atmosphere. Each product alloy button was melted five times, on alternate sides, in order to increase homogeneity. After the arc melting process, measurements were performed on the as-cast $x = 0.05$ series. The $x = 0.10$ compounds were wrapped in tantalum foil and sealed in an evacuated quartz glass ampule for annealing at a temperature $T_A = 1050^\circ C$ for three days. To minimize any phase transitions from gradual cooling after furnace shutoff, the ampule was promptly quenched in $58^\circ F$ chilled water, passing from T_A to room temperature ($75^\circ F$) in a very short time. A portion of each compound was ground to $75 \mu m$ size powder for X-ray diffraction (XRD) crystallography. A Siemens D500 diffractometer with $Cu K\alpha$ radiation was used for XRD analysis. AC magnetic susceptibility (χ_{AC}) was performed using a Princeton Applied Research model 5210 lock-in amplifier with an AC magnetic susceptometer constructed in our laboratory. Several of the samples were further tested using a Quantum Design DC SQUID magnetometer.

III. RESULTS AND DISCUSSION

A. Crystal Structure

We calculated the Miller indices for the powder diffraction pattern of our YNi_2B_2C sample. X-ray angle 2θ in degrees ($^\circ$), lattice plane spacing d (in angstrom units \AA), Miller index values (hkl), and measured relative intensity I/I_0 (in %) where I_0 is the intensity of the highest line are shown in Table I below for each line of this parent compound. The highest XRD intensity I_0 occurs at a Miller index of (112). The measured XRD intensities I in Figures 1 and 2 are given in counts per second (cps).

Table I X-ray Angle, Lattice Spacing, Miller Index, and Relative Intensity for YNi_2B_2C

$2\theta(^\circ)$	$d(\text{\AA})$	(hkl)	I/I_0 (%)
26.60	3.3482	(101)	31
33.89	2.6425	(004)	45
35.95	2.4961	(110)	33
35.98	2.4937	(103)	33
39.91	2.2570	(112)	100
50.24	1.8145	(114)	1
50.26	1.8136	(105)	8
51.75	1.7650	(200)	16
54.79	1.6741	(202)	<1
59.12	1.5613	(211)	6
63.31	1.4677	(204)	18
64.64	1.4407	(213)	21

Some minor secondary phases were evident as 3d transition metal content x went from 0.05 to 0.10 in the daughter compounds. Compositions $T = Fe$ and Co at $x = 0.05$, and $T = Cu$ at $x = 0.10$ had the lowest proportion of such phases while $T = Zn$ had a markedly different structure.

Figure 1 on the next page contains the X-ray diffraction spectra with Miller indices for $YNi_{2-x}Fe_xB_2C$ and Figure 2 has the same for $YNi_{2-x}V_xB_2C$. Carbon, nickel yttrium, metal carbides, metal borides, and metal borocarbides were secondary phase components present in small amounts in the substituted compounds. With regard to the formation of YNi_xB_xC with

$x \in \{2, 3, 4, 5\}$, we observed preservation of the main $\text{YNi}_2\text{B}_2\text{C}$ spectral lines in $\text{YNi}_3\text{B}_3\text{C}$ with evident breaking of the structure in $\text{YNi}_4\text{B}_4\text{C}$.

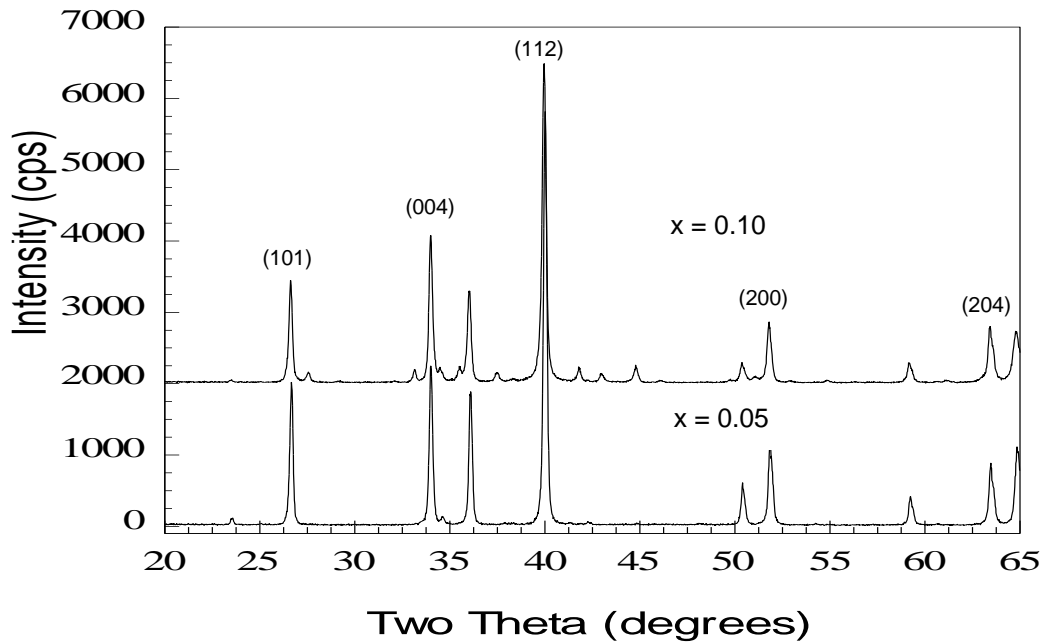


Figure 1. X-ray diffraction spectra for $\text{YNi}_{2-x}\text{Fe}_x\text{B}_2\text{C}$ with $x = 0.05$ and 0.10 . Not all indices have been shown due to space limitations; refer to Table I.

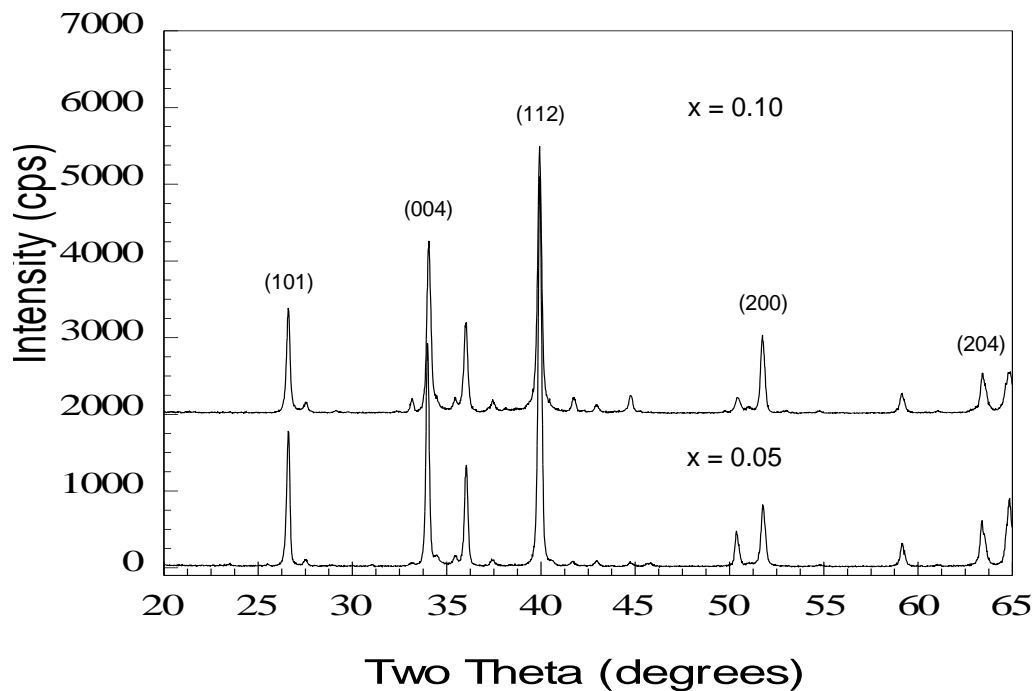


Figure 2. X-ray diffraction spectra for $\text{YNi}_{2-x}\text{V}_x\text{B}_2\text{C}$ with $x = 0.05$ and 0.10 . Not all indices have been shown due to space limitations; refer to Table I.

B. Magnetic Properties

It is well established that one of the fundamental properties of a superconductor is diamagnetism at T_C [6, 7]. All samples therefore had AC magnetic susceptibility χ_{AC} measurements in arbitrary units (a.u.) versus temperature in Kelvin units (K). Table II on the next page summarizes pertinent data from the χ_{AC} measurements. The critical temperature of the onset transition is T_C . Substitution by ferromagnetic Fe significantly lowered T_C . Some of the samples also had magnetization measurements in electromagnetic units per gram (emu/g) versus temperature in Kelvin units (K) made by a SQUID DC magnetometer.

Table II Radius r , magneton number μ , and T_C for $\text{YNi}_{2-x}\text{T}_x\text{B}_2\text{C}$ ($x = 0.05$ and 0.10)

Element T	Ti	V	Cr	Mn	Fe	Co	Cu	Zn
r (Å)	1.32	1.22	1.18	1.17	1.17	1.16	1.17	1.25
μ (+2) [†]	--	3.8	4.8	5.9	5.4	4.8	1.9	--
μ (+3) [‡]	--	2.8	3.7	5.0	5.9	--	--	--
T_C (K) $x = 0.05$	15.8	17.9	16.1	15.2	10.7	14.5	16.5	--
T_C (K) $x = 0.10$	16.3	15.8	15.7	15.8	7.3	15.0*	14.7	--

[†] μ (+2) is the divalent ion effective Bohr magneton number.

[‡] μ (+3) is the trivalent ion effective Bohr magneton number.

* A second transition occurs at 11 K.

Our as-cast $\text{YNi}_2\text{B}_2\text{C}$ sample showed a diamagnetic transition at 15.8 K in AC magnetic susceptometry, near the 15.6 K T_C value reported for an annealed sample's DC electrical resistivity [1]. As $T = \text{Ti}$ and Mn content x went from 0.05 to 0.10, a small increase in T_C was observed. Other 3d metal substitutions had decreasing T_C with increasing x , except for ferromagnetic $T = \text{Co}$ at $x = 0.10$, which had two transitions. Two phases likely exist in that sample, with the Co-rich phase producing a lower T_C much as $T = \text{Fe}$ did. The largest 3d ions had various effects. Annealed Ti and V ($x = 0.10$) samples showed some evidence for multiphase magnetic transitions from a superposition of two crystal phases, whereas the $x = 0.05$ Zn substitution produced no magnetic transition in the measurement region. Zn has a filled 3d subshell like the smaller Cu ion but its larger ionic size distorts the crystal structure markedly.

Figure 3 below shows χ_{AC} versus temperature measurements for the sample $T = \text{Fe}$ with $x = 0.05$. The critical temperature T_C is near 10.7 K as can be seen in the figure.

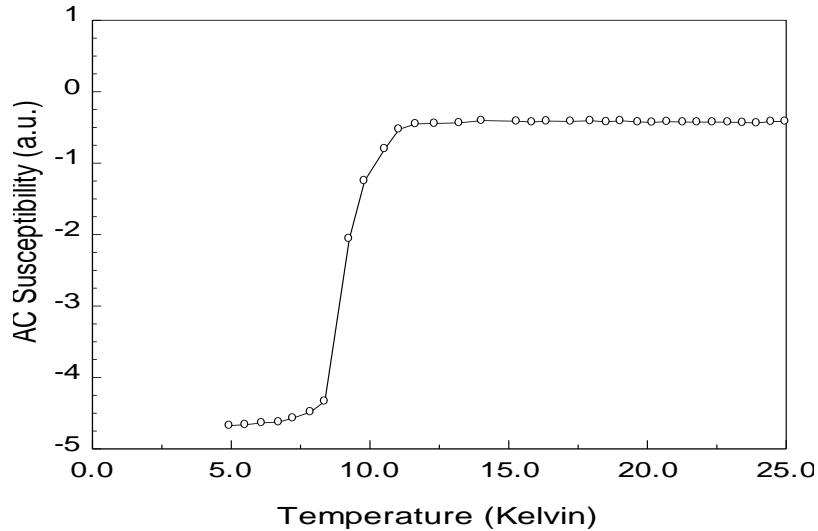
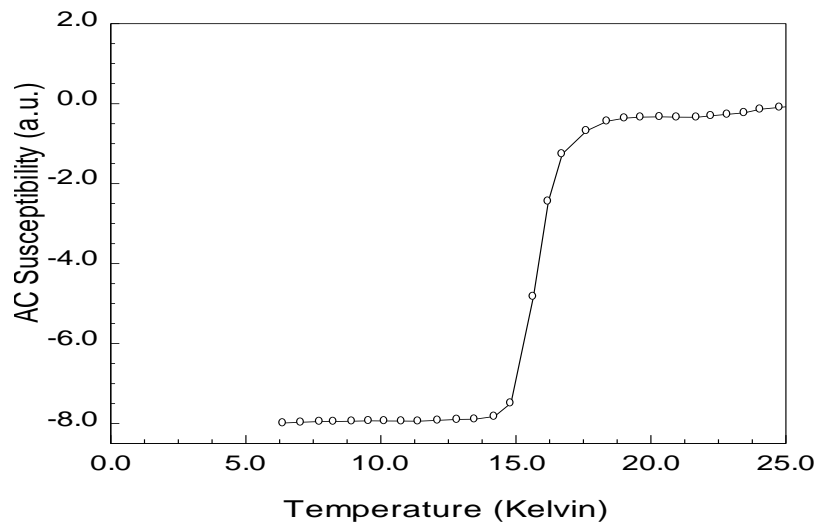
**Figure 3.** AC magnetic susceptibility for $\text{YNi}_{2-x}\text{Fe}_x\text{B}_2\text{C}$ with $x = 0.05$.

Figure 4 shows χ_{AC} versus temperature for the sample $T = \text{V}$ with $x = 0.05$. The critical temperature T_C is near 17.9 K as can be seen in the figure.

**Figure 4.** AC magnetic susceptibility for $\text{YNi}_{2-x}\text{V}_x\text{B}_2\text{C}$ with $x = 0.05$.

The SQUID magnetometer measurements of magnetization versus temperature were made with an applied DC field of 500 gauss (G). (Our AC magnetic probe produced a much smaller AC magnetic field.) All the samples we measured except for T = Zn clearly exhibit the magnetic behavior of type II superconductors [6, 7]. When first cooled in zero field (ZFC), they then show magnetic shielding or flux expulsion when a field is applied. When cooled below T_C in an applied field, they show flux entrapment. The as-cast $YNi_{1.95}V_{0.05}B_2C$ sample (Figure 6) showed a diamagnetic transition at 13.8 K. We also noted diamagnetic transitions in the YNi_3B_3C , YNi_4B_4C , and YNi_5B_5C compounds. As-cast YNi_2B_2C (Figure 5) and YNi_4B_4C had transitions corresponding to $T_C = 13$ K and 14 K, respectively. We also measured an as-grown crystal of YNi_2B_2C , made in our Centorr tri-arc furnace under a flowing argon atmosphere using the Czochralski process, and it had a $T_C \approx 14$ K.

We see in our data evidence for substituted 3d ion creation of local scattering centers which reduce the T_C of the parent compound's superconductivity. Non-ferromagnetic or lower magneton number 3d ions did not affect T_C as much as ferromagnetic Fe although there are also ion size and electron orbital occupation factors to consider, the latter factors perhaps accounting for the observed absence of superconductivity in Zn over our temperature measurement range ≥ 5 K.

Figure 5 below shows magnetization versus temperature in YNi_2B_2C using a magnetizing field $H = 500$ G.

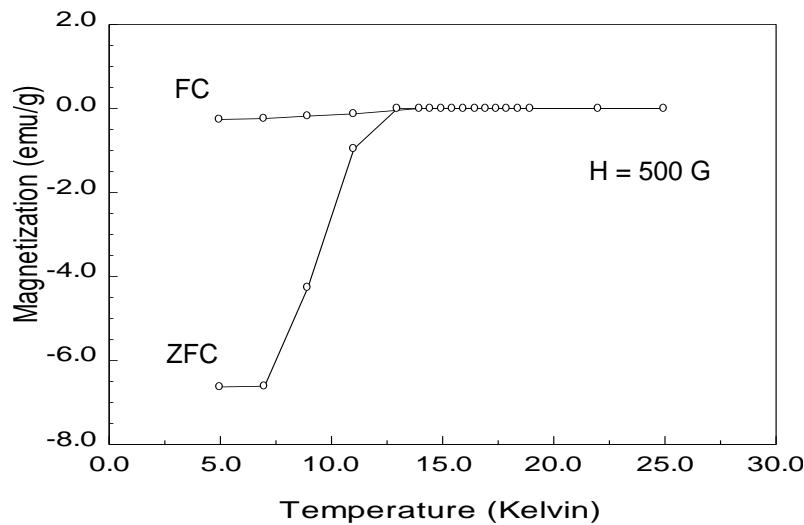


Figure 5. Magnetization versus temperature for YNi_2B_2C .

Again, ZFC in these plots refers to cooling in zero magnetic field (with the magnetic field subsequently applied) and shows magnetic flux expulsion, a characteristic of a superconductor. Note that cooling in the presence of a magnetic field results in flux entrapment. The divergence between ZFC and field cooling (FC) appears to be at 12.5 K.

Figure 6 below shows magnetization versus temperature in $YNi_{2-x}V_xB_2C$ with $x = 0.05$ using a magnetizing field $H = 500$ G.

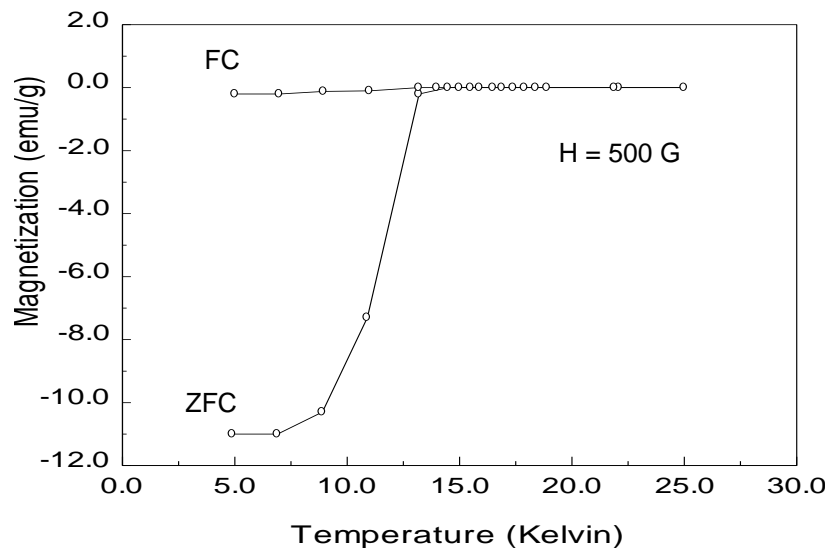


Figure 6. Magnetization versus temperature for $YNi_{2-x}V_xB_2C$ with $x = 0.05$.

The divergence between ZFC and FC again appears to be at 12.5 K. This also reflects the value of the critical temperature T_c where the sample begins to exhibit perfect diamagnetism.

While these metallic Y-Ni-B-C materials are classified as low T_c superconductors, they do share certain advantageous features of other low T_c superconductors such as Nb_3Ge [8] and MgB_2 . Metal alloy superconductors are malleable and ductile, not brittle like the ceramic (cuprate) types, and thus can be easily formed into long wires and thin foils.

REFERENCES

- [1] Cava, R. J., Takagi, H., Zandbergen, H. W., Krajewski, J.J., Peck, Jr, W. F., Siegrist, T., Batlogg, B., van Dover, R. B., Felder, R. J., Mizuhashi, K., Lee, J. O., Eisaki, H., & Uchida, S. *Superconductivity in the quaternary intermetallic compounds $\text{LnNi}_2\text{B}_2\text{C}$* . Nature, **367**, 252-253 (1994).
- [2] Cava, R. J., Takagi, H., Batlogg, B., Zandbergen, H. W., Krajewski, J. J., Peck, Jr, W. F., van Dover, R. B., Felder, Siegrist, T., R. J., Mizuhashi, K., Lee, J. O., Eisaki, H., Carter, S. A. & Uchida, S. *Superconductivity at 23 K in yttrium palladium boride carbide*. Nature, **367**, 146-148 (1994).
- [3] Nagarajan, R., Mazumdar, C., Hossain, Z., Dhar, S. K., Gopalakrishnan, K. V., Gupta, L.C., Godart, C., Padalia, B. D., & Vijayaraghavan, R. *Bulk Superconductivity at an Elevated Temperature ($T_C \approx 12\text{K}$) in a Nickel Containing Alloy System Y-NiB-C* . Physical Review Letters, **72**, 274-277 (1994).
- [4] Mazumdar, C., Nagarajan, R., Godart, C., Gupta, L. C., Latroche, M., Dhar, S. K., Levy-Clement, C., Padalia, B. D., and Vijayaraghavan, R. *Superconductivity at 12 K in Y-Ni-B System*. Solid State Communications, 87, 413-416 (1993).
- [5] Siegrist, T., Zandbergen, H. W., Cava, R. J., Krajewski, J.J., & Peck, Jr, W. F. *The crystal structure of superconducting $\text{LuNi}_2\text{B}_2\text{C}$ and the related phase LuNiBC* . Nature, **367**, 254-256 (1994).
- [6] Ashcroft, N. W. & Mermin, N. D. *Solid State Physics*, W. B. Saunders, 1976.
- [7] Ginzburg, V. L. & Andryushin, E. A. *Superconductivity*, World Scientific, 1994.
- [8] Serway, R. & Jewett, Jr, J. *Physics for Scientists and Engineers*, 10th Edition, Cengage Learning, 2019.